OXFORD

Carcinogenesis, 2015, Vol. 36, No. 5, 564–573

doi:10.1093/carcin/bgv041
Advance Access publication March 30, 2015
Original Manuscript

ORIGINAL MANUSCRIPT

17β-estradiol inhibits spreading of metastatic cells from granulosa cell tumors through a non-genomic mechanism involving GPER1

Charlotte M.François[1,2,3], Richard Wargnier[1,2,3], Florence Petit[1,2,3], Thibaut Goulvent[4,5], Ruth Rimokh[4], Isabelle Treilleux[6], Isabelle Ray-Coquard[7], Valeria Zazzu[8], Joëlle Cohen-Tannoudji[1,2,3] and Céline J.Guigon[1,2,3,*]

[1]INSERM U1133, Physiologie de l'Axe Gonadotrope, F-75013 Paris, France, [2]Université Paris Diderot, Sorbonne Paris Cité, Biologie Fonctionnelle et Adaptative, F-75013 Paris, France, [3]CNRS UMR 8251, Biologie Fonctionnelle et Adaptative, F-75013 Paris, France, [4]U1052 INSERM, UMR CNRS 5286, Université de Lyon, Centre de Recherche en Cancérologie de Lyon, Centre Léon Bérard, Lyon F-69000, France, [5]Institut Roche de Recherche et Médecine Translationnelle, 92650 Boulogne Billancourt, France, [6]Department of Pathology, Centre Léon Bérard, Lyon F-69000, France, [7]Department of Medical Oncology, Centre Léon Bérard, Université de Lyon, Lyon F-69000 and GINECO Group, Paris, France and [8]Institute of Genetics and Biophysics "A. Buzzati-Traverso"-CNR, I-80131 Naples, Italy

*To whom correspondence should be addressed. Unité de Biologie Fonctionnelle et Adaptative, 4 rue MA Lagroua Weill-Hallé, F-75013 Paris, France. Tel: +33 1 57 27 84 04; Fax: +33 1 57 27 84 14; Email: celine.guigon@univ-paris-diderot.fr

Abstract

Granulosa cell tumor (GCT) is a rare and severe form of sex-cord stromal ovarian tumor that is characterized by its long natural history and tendency to recur years after surgical ablation. Because there is no efficient curative treatment beyond surgery, ~20% of patients die of the consequences of their tumor. However, very little is known of the molecular etiology of this pathology. About 70% of GCT patients present with elevated circulating estradiol (E2). Because this hormone is known to increase tumor growth and progression in a number of cancers, we investigated the possible role of E2 in GCTs. Cell-based studies with human GCT metastases and primary tumor-derived cells, ie KGN and COV434 cells, respectively, aimed at evaluating E2 effect on cell growth, migration and invasion. Importantly, we found that E2 did not affect GCT cell growth, but that it significantly decreased the migration and matrix invasion of metastatic GCT cells. Noteworthy, our molecular studies revealed that this effect was accompanied by the inhibition through non-genomic mechanisms of extracellular signal-regulated kinase 1/2 (ERK1/2), which is constitutively activated in GCTs. By using pharmacological and RNA silencing approaches, we found that E2 action was mediated by G protein-coupled estrogen receptor 1 (GPER1) signaling pathway. Analyses of GPER1 expression on tissue microarrays from human GCTs confirmed its expression in ~90% of GCTs. Overall, our study reveals that E2 would act via non-classical pathways to prevent metastasis spreading in GCTs and also reveals GPER1 as a possible target in this disease.

Introduction

Granulosa cell tumors (hereafter referred to as GCTs) are sex-cord stromal tumors which account for ~5% of ovarian tumors. This disease can affect women of all ages, with two distinct clinical presentations, the adult and the juvenile forms (1). Most juvenile cases are diagnosed early and their prognosis is generally good, though recurrences and metastases have been reported. However, in the adult cases of GCT, 20% of patients die of the consequences of their tumor, with a 5-year survival of advanced oncological

Received: October 28, 2014; **Revised:** March 5, 2015; **Accepted:** March 23, 2015

Abbreviations

CD-FBS	charcoal-dextran stripped fetal bovine serum
DAPI	4′,6-diamidino-2-phenylindole
DMSO	dimethyl sulfoxide
DMEM	Dulbecco's modified Eagle's medium
DPBS	Dulbecco's phosphate-buffered saline
DPN	2,3-bis(4-hydroxyphenyl)propionitrile
E2	estradiol
ERK1/2	extracellular signal-regulated kinase 1/2
ER	estrogen receptors
FBS	fetal bovine serum
GCT	granulosa cell tumor
GPCR	G protein-coupled receptor
GPER1	G protein-coupled estrogen receptor 1
HA	hemagglutinin
MAPK	mitogen-activated protein kinase
MEK1/2	MAP ERK kinases 1/2
MPP dihydrochloride	1,3-*Bis*(4-hydroxyphenyl)-4-methyl-5-[4-(2-piperidinylethoxy)phenol]-1H-pyrazole dihydrochloride
MTT	(3-(4,5-dimethylthiazole-2-yl)-2,5-diphenyl tetrazolium bromide)
PI3K	phosphatidyl-inositol 3 kinase
PPT	1,3,5-Tris(4-hydroxyphenyl)-4-propyl-1H-pyrazole
shRNA	small hairpin RNA
TMA	tissue micro-array

stage patients being less than 50% (1). These tumors have a tendency to late recurrence, with latency after primary tumor treatment of up to 37 years. Chemotherapy has limited success, and surgery remains the main therapeutic approach (2).

Despite the importance and insidiousness of GCT, very little is known of its molecular etiology. In an effort to identify a specific marker of adult GCTs, Shah and collaborators (3), however, discovered a single recurrent somatic mutation in a Forkhead transcription factor, *FOXL2*, in 97% of GCT samples from adult patients (Cys134Trp). This mutation may reduce sensitivity to apoptosis and stimulate proliferation of granulosa cells (4,5). It may also contribute to overstimulate estradiol (E2) production, a feature that is observed in 70% of patients, through increased expression of the enzyme converting androgens into estrogens, ie CYP19 aromatase (6,7). Discovery of the *FOXL2* mutation has also brought new tools for improving the diagnosis of GCTs (8).

In addition to E2, GCTs produce increased amounts of inhibin B and anti-Müllerian hormone, which are both used as serum markers for the diagnosis (9,10). However, the hormone that is responsible for most of the clinical signs of GCT, including abnormal uterine bleeding, endometrial hyperplasia and adenocarcinoma is E2 (11). This hormone, which is mainly produced by the ovary, is known to mediate important physiological responses by binding to nuclear estrogen receptors (ER), ERα and ERβ. In the ovary, it plays a key role by regulating follicular growth and ovulation (12,13). Although the expression of ERs is maintained in GCTs, repression of ER signaling by the transcription factor nuclear factor-kappaB (NF-κB) prevents ER-mediated transcription in GCTs, indicating that nuclear E2 signaling would not be functional in these tumors (14). On the other hand, alternative mechanisms of action of E2 that have been demonstrated in other models have not been evaluated in this type of tumor. Indeed, in addition to regulating gene transcription, the existence of non-genomic mechanisms whereby ERs interact with and regulate the activity of protein kinases has been demonstrated in cell-based studies but also *in vivo* (15).

The present report aims at examining the effect of E2 on the growth and metastatic potential of GCT and its molecular mechanisms of action. Through cell-based studies, we demonstrated that E2 inhibited the migration and invasion capabilities of metastatic granulosa cells without affecting cell growth. Our molecular studies revealed that E2 rapidly decreased the activity of extracellular signal-regulated kinase 1/2 (ERK1/2) signaling via non-genomic mechanisms through a non-classical ER belonging to the G protein-coupled receptor (GPCR) family, GPER1 (for G protein-coupled estrogen receptor, or GPR30) (16). We found this receptor to be expressed in about 90% of human GCT samples spotted on tissue microarrays (TMAs). Overall, our study provides new insights about the possible role and mechanism of action of E2 in GCTs and reveals GPER1 signaling as being a possible target in this disease.

Materials and methods

Reagents and plasmids

Reagents used in this study are described in Supplementary Materials and methods, available at *Carcinogenesis* Online. The plasmid pTL1-HA2-GPER1 was obtained by amplification of human GPER1 from the plasmid pcDNA3-GPER1-EGFP, kindly provided by Prof. Eric Prossnitz (University of New Mexico, Albuquerque), using the following PCR primers: forward 5′–CCCAAGCTTGCCACCATGGATGTGACTTCC–3′ and reverse 5′–TAGT TTAGCGGCCGCACGTTAGCACCTGCATTACCTACACGGCACTGCTG–3′ with the Pfx50 DNA polymerase. The product was purified (QIAquick PCR purification, Qiagen, Venlo, the Netherlands), cut with HindIII and NotI and ligated with T4 DNA ligase into the plasmid pTL1-HA2. The empty plasmid pTL1-HA-mcs1 was obtained by cutting pTL1-HA2-GPER1 with NotI and BamHI and ligation with a dimer composed of 5′– GATCCCTGCAGGACC GGTCTCGAGAAGCTTACGCGTACTAGTGC–3′ and 5′–GGCCGCACTAGT ACGCGTAAGCTTCTCGAGACCGGTCCTGCAGG–3′. GPER1-specific and negative control small hairpin RNA (shRNA) plasmids carrying a puromycin resistance gene were obtained from QIAGEN (#336314KH11263P, SureSilencing shRNA).

Cell lines

The KGN cell line is a metastatic granulosa cell line established from an adult patient with recurrent, metastasized GCT in the pelvic region (17). It harbors the *FOXL2 C402G* mutation described in most adult GCTs. It was purchased in 2011 from the RIKEN BioResource Center (RBRC-RCB1154, RIKEN Cell Bank, Ibaraki, Japan) after approval by Drs Yoshiro Nishi and Toshihiko Yanase. COV434 cells, derived from a primary tumor of a 27-year-old patient (18), harbor the wild-type *FOXL2* gene but its expression is low to absent (19). They originated from ECACC (#07071909, Sigma–Aldrich), kindly provided at passage 2 by Pr Reiner Veitia (Institut Jacques Monod, University Paris 7, France). These two human GCT cell lines are particularly suitable as models of GCT cells since they have genetic and molecular alterations found in GCTs, and they retain characteristics of granulosa cells (17,20). Upon receipt, cells were immediately tested for a number of markers found in granulosa cells, such as ERs (Supplementary Figure 1, available at *Carcinogenesis* Online), CYP19 aromatase and follicle-stimulating hormone receptor using RT–PCR (reverse transcription–polymerase chain reaction) and/or western blots (data not shown). They were routinely maintained at 37°C with 5% CO_2 in Dulbecco's modified Eagle's medium (DMEM)/F12 containing 10% fetal bovine serum (FBS) and 0.5% penicillin/streptomycin. MCF7 cells were purchased from ATCC in 2010 (HTB-22, generously provided at passage 2 by Dr Ait-Si-Ali, CNRS UMR7216, University Paris Diderot). They were grown in DMEM containing 5% FBS and 0.5% PS. For experiments, cells were cultured in medium without phenol red and charcoal-dextran stripped fetal bovine serum (CD-FBS). Only cells at early passage (<25) were used for the experiments.

GCT cell growth

For MTT (3-(4,5-dimethylthiazole-2-yl)-2,5-diphenyl tetrazolium bromide) assay, cells were seeded at a density of 1×10^5 cells per well in 12-well plates in 10% CD-FBS growth medium. Twenty-four hours later, they received the indicated treatment. At each studied time (0, 24, 48 and 72 h), cells were incubated with MTT (1 mg/ml in Dulbecco's phosphate-buffered saline [DPBS]) for 2.5 h, and then lysed in dimethyl sulfoxide (DMSO). The

absorbance was read at 575 nm with FlexStation3 (Molecular Devices). The experiments were run at least three times.

GCT cell migration

Cell migration was performed as described (21) with some modifications. Before seeding cells, a starting line was drawn in the middle of a well from a 6-well plate with a surgical blade. Cells were seeded at a density of 4×10^5 cells/well in complete growth medium. Twenty-four hours later, the medium was replaced by DMEM/F12 medium containing 10% CD-FBS. The day after, cells at the right side of the starting line were swept away with a cell lifter. Cells were gently washed with DPBS, and then 2 ml of DMEM/F12 medium containing 10% CD-FBS with gelatin (1 mg/ml) were added. Ara-C (10 µM), a selective inhibitor of DNA synthesis was used to prevent cell proliferation. Cells were then treated with the test substance or their respective vehicle (time 0). Migration was monitored by phase-contrast microscopy. For each well, three digital images of the front line were taken at time 0 and 24 h, and the migration distance was established by measuring the distance of the front line at time 0 and 24 h, using Photoshop CS3. Front line at 24 h was defined as a virtual line constituted by at least three aligned cells. Three or more independent experiments were performed.

Matrigel invasion

The day before the assay, the growth medium was replaced by serum-free medium. Transwell inserts were rehydrated with DMEM/F12 containing 0.2% CD-FBS, coated with 100 µg Matrigel and then left at 37°C for 24 h. On the day of the experiment, they were rinsed with DMEM/F12 containing 0.2% CD-FBS. Bottom wells were filled with 10% CD-FBS DMEM/F12 medium. KGN cells were harvested by mild trypsinization and seeded at a density of 2×10^5 cells/transwell in 0.2% CD-FBS DMEM/F12 medium in the presence of the indicated drugs (time 0). After 4.5 h, cells were rinsed in DPBS and then fixed in 4% paraformaldehyde for 20 min at room temperature. They were rinsed in DPBS and their nuclei were stained by 4′,6-diamidino-2-phenylindole (DAPI). Cells located on the inner side of the transwell (non-invading cells) were removed with a cotton swab. Membranes were detached from transwells with a surgical blade and mounted on glass slides to observe the invading cells on the outer side of the transwell with a fluorescence microscope (Nikon Eclipse 90i). For each transwell, three different fields were photographed at ×10 magnification. Cell counting was performed using ImageJ software (NIH, 1.64 version).

Western blot

Cells were seeded at a density of 1×10^6 cells per 60-mm Petri dish, or at 5×10^5 cells par well in 6-well plates and grown in DMEM-F12 with 10% FBS. After 24 h, they were incubated in a phenol red-free medium with 10% CD-FBS for at least 24 h. Cells were then incubated with different treatments for the indicated times. Whole cell lysates were prepared as described previously (22). Membranes were incubated in 10% milk for 15 min and incubated overnight with primary antibodies at 4°C. The following day, they were incubated with an anti-rabbit horseradish peroxidase-linked IgG antibody (dilution: 1/3000) for 2 h. Proteins were detected by chemiluminescence with enhanced chemiluminescence using charge coupled device camera (LAS 4000, FujiFilm). The ratios of phosphorylated to total levels of proteins were established by quantification with ImageJ software.

GPER1 subcellular localization by confocal microscopy

Cells were seeded in 8-well Labtek chambers at a density of 4×10^4 cells per well. After 24 h, the medium was replaced by phenol red-free medium with CD-FBS for 24 h. Cells were incubated overnight at 4°C with rabbit anti-GPER1 antibody (Sigma, 1/100) alone or in the presence of mouse anti-calnexin (1/1000) antibody diluted in phosphate buffered saline with bovine serum albumin 1%-triton 0.1%. After rinsing with phosphate-buffered saline, cells were incubated with secondary mouse and rabbit antibodies coupled to fluorochromes (dilution: 1/3000). GPER1 immunostained cells were incubated with phalloidin–fluorescein isothiocyanate (dilution: 1/100) for 1 h to visualize actin cytoskeleton. Nuclear staining was obtained after staining with DAPI. Images were captured using a motorized confocal laser scanning microscope (LSM 700; Carl Zeiss SAS, Le Pecq, France).

Hemagglutinin (HA)-GPER1 transfection and immunofluorescence

Cells were seeded at a density of 6×10^4 cells per well in 8-well Lab Tek chamber slide. On the next day, they were transfected with 150 ng of the backbone pTL1-HA-mcs1 or pTL1-HA2-GPER1 using lipofectamine 2000 (ratio 1:3) and OptiMEM. Transfections were conducted according to manufacturer's instructions. After 6 h, transfection medium was replaced by phenol red-free medium, containing 10% FBS and 0.5% penicillin–streptomycin. On the next day, cells were processed for immunofluorescence. After washing in DPBS, cells were fixed for 20 min in 4% paraformaldehyde at room temperature. They were then permeabilized during 30 min with phosphate buffered saline with bovine serum albumin 1%–triton 0.1%. For HA-GPER1 immunodetection, cells were incubated overnight at 4°C with rabbit anti-GPER1 antibodies (Sigma or LS4271 at a 1/100 and 1/500 dilution, respectively) and mouse anti-HA antibody (dilution: 1/200). The next day, cells were rinsed and incubated for 2 h with anti-mouse and anti-rabbit secondary antibodies (dilution: 1/1000). They were then stained with DAPI, mounted on a glass slide and observed under a fluorescence microscope (Nikon Eclipse 90i).

GPER1 silencing

KGN cells were transfected by electroporation (Neon system, Invitrogen Corp.) using GPER1-specific and negative control shRNAs, following manufacturer's instructions. Briefly, 6×10^5 cells were mixed with 1 µg linearized plasmids and electroporated at 1500V for 30 ms using 100 µl Neon Tips (#MPK1009). They were then seeded in a well of a 6-well plate. Six hours after electroporation, they were incubated in 10% FBS growth medium. Two days after transfection, cells were diluted 10-fold in 24-well plates in selecting 10% FBS growth medium containing 0.2 µg/ml puromycin. They were cultured for 6 weeks in selecting medium. Two different negative control and two shGPER1 stable cell clones were used for the experiments. Efficient knockdown of GPER1 was checked by real-time RT-PCR, as described in Supplementary Materials and methods, available at *Carcinogenesis* Online.

Tumor samples, TMA and GPER1 immunohistochemistry

The adult GCTs included in this study were independently reviewed by two different pathologists and were collected through the National Rare Ovarian Tumor Observatory (TMRO) developed by the Group of National Investigators for Ovarian Cancer Studies (GINECO) (23). Analysis of *FOXL2 C402G* mutation was assessed, as described (8).

The expression of GPER1 was assessed following two criteria: staining intensity (0: no staining; 1: weak; 2: intermediate; 3: strong) and percentage of stained cells. The immunoreactivity score was obtained by multiplication of staining intensity and percentage of stained cells. Additional information can be found in Supplementary Materials and methods, available at *Carcinogenesis* Online.

Statistical analyses

All data were analyzed using Prism 6 (version 6.0, GraphPad Software). In cell-based studies, statistical analyses were performed using Student's *t*-test and one- or two-way analysis of variance depending on the experimental setting. The data of TMA were analyzed using Student's *t*-test and Pearson correlation. When appropriate, data are shown as means ± SEM. A two-tailed P value < 0.05 was considered as significant.

Results

17β-estradiol has no effect on cell growth, but it inhibits the migration and invasion of metastatic granulosa cells

We first examined the possible effect of E2 on the growth of two human ER-positive GCT cell lines, ie COV434 and KGN cells established from a primary tumor and a metastatic recurrence, respectively. No effect of E2 (10 nM) was observed on both cell lines after 24, 48 or 72 h by MTT assays (Figure 1A a and b). Either lower (100 pM) or higher doses of E2 (up to 1 µM) did not induce any change in cell growth (data not shown). Similar results were obtained when cells were numerated with an automatic cell counter (data not shown).

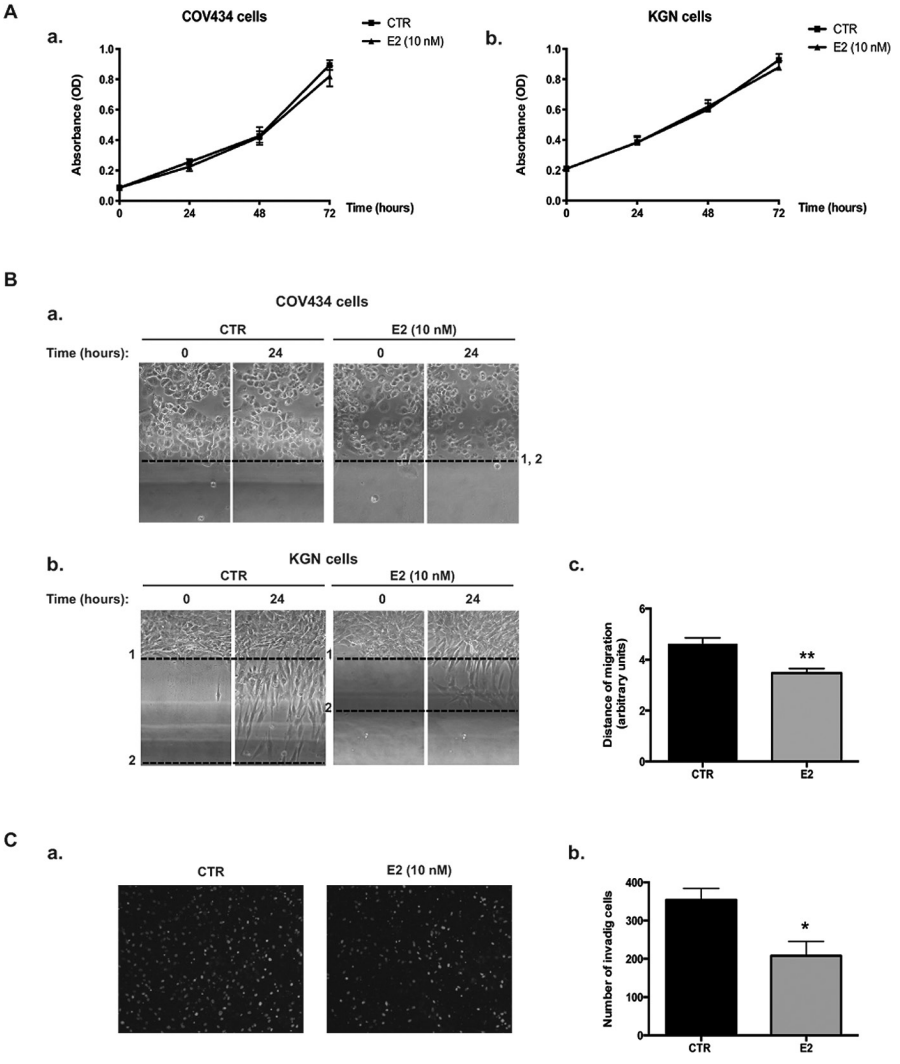

Figure 1. E2 treatment has no effect on the growth of the two GCT cell lines, COV434 and KGN cells, but it represses KGN cell migration and invasion capabilities. (**A**) MTT assays on COV434 (a) or KGN (b) cells treated for the indicated times with E2. (**B**) Bi-dimensional horizontal migration assays with COV434 (a) or KGN (b) cells treated for 24 h with vehicle (control, CTR) or E2. KGN and COV434 cells were scraped from the culture dish and the mean migration distance of cells was assessed after 24 h, as indicated in Materials and methods. Positions of the front lines at time 0 and 24 h are shown on representative images as dotted lines (1 and 2, respectively). No migration is observed for COV434 cells after 24 h. In control (CTR) conditions, KGN cells have the capability to migrate. (c) Quantification of the migration distance for KGN cells is shown as means ± SEM in bar graphs. (**C**) Matrigel invasion assays of KGN cells. (a) Representative images of invading cells 4.5 h after vehicle (CTR) or E2 treatment. (b) Quantification of the number of invading cells is shown as means ± SEM in bar graphs. $^{*}P < 0.05$, $^{**}P < 0.01$ versus CTR.

We next assessed the possibility that E2 could alter the migration of GCT-derived cell lines, by performing bi-dimensional horizontal migration assays (Figure 1B). In control conditions, we observed that metastatic KGN cells had the ability to migrate, whereas the primary tumor-derived COV434 cells did not (Figure 1B a and b). Importantly, E2 induced a significant decrease in KGN cell migration after 24 h, with a reduction of ~25% in their migration distance (Figure 1Bb and c). To test the effect of E2 on the capability of KGN cells to invade, we performed invasion assays using matrigel-coated transwells. In control conditions, KGN cells could efficiently invade the matrix to migrate through the pores of the transwell, as illustrated in Figure 1Ca. E2 treatment impaired KGN cell invasion as shown by the significant reduction of ~40% in the number of invading cells (Figure 1Cb).

17β-estradiol regulates the activity of ERK1/2 through non-genomic actions

We next searched for the molecular mechanism underlying E2 action in metastatic granulosa cells. Previous works have shown that in GCT-derived cell lines including KGN cells, endogenous or transfected ERα and ERβ are unable to transactivate an estrogen-responsive reporter construct in luciferase assays (14). We, thus, examined whether E2 could mediate its action on cell migration and invasion through rapid, non-genomic regulation of kinase pathways. In particular, we studied the activity of the mitogen-activated protein kinase (MAPK) and phosphatidyl-inositol 3 kinase (PI3K)/Akt pathways, which are rapidly regulated by ERs in a number of cell lines such as in the breast cancer MCF7 cells (24–26) used as controls in the present study.

KGN and MCF7 cells were treated for 10 and 60 min with or without E2, and the activity of MAPK and PI3K/Akt pathways was analyzed by western blots with antibodies recognizing the phosphorylated and total (phosphorylation state-independent) forms of MAPK family members, ie ERK1/2, p38 and c-jun N-terminal kinase (JNK), and of a downstream target of PI3K, ie Akt. In KGN cells, there was a ≈30% decrease in the phosphorylation of ERK1/2 protein levels after 10 and 60 min of E2 treatment, whereas there was no alteration in total ERK1/2 abundance

(Figure 2Aa). Concomitantly, there was no change in the ratios of phosphorylated to total levels of p38 MAPK (Figure 2Ab). Phosphorylated JNK could be barely detected in KGN cells (data not shown). No change in the ratios of phosphorylated to total Akt was detected (Figure 2Ac). Consistent with previous observations, in MCF7 cells there was a rapid increase in the ratios of phosphorylated to total ERK1/2 protein levels and of those of p38 MAPK upon E2 treatment (Supplementary Figure 1A and B, available at *Carcinogenesis* Online). No change was observed in the phosphorylation of Akt or JNK (Supplementary Figure 1C, available at *Carcinogenesis* Online and data not shown).

Time course studies were performed in KGN cells to evaluate the alterations in ERK1/2 activity occurring after E2 treatment. The decrease in ERK1/2 activity was apparent as soon as 5 min of E2 incubation treatment and lasted up to 24 h (Figure 2B). We also assessed whether E2-mediated repression of ERK1/2 activity occurred via inhibition of the Ras/Raf pathway. To address this question, we studied by western blot the activity of MAP ERK kinases 1/2 (MEK1/2), which drive ERK1/2 phosphorylation in this signaling pathway. Interestingly, there was no change in MEK1/2 phosphorylation after E2 treatment (Figure 2C), suggesting that E2-induced decrease in ERK1/2 activity did not involve any alteration of Ras/Raf signaling.

Pharmacological inhibition of ERK1/2 activity by U0126 reduces cell migration and invasion of metastatic granulosa cells

Constitutive activation of ERK1/2 signaling pathway has been previously reported in GCTs (27). However, to our knowledge the effect of ERK1/2 inhibition in GCT cell lines on their capability to migrate or to invade has never been evaluated. To determine whether the decrease in ERK1/2 activity in metastatic KGN cells could lead to the reduction of their migration and invasion capabilities, we studied the effect of selective ERK1/2 repression by the MEK1/2 inhibitor U0126. As expected, there was a dose–response effect on the ratios of phosphorylated to total ERK1/2 levels studied by western blot (Figure 3A). Bi-dimensional horizontal migration assays showed that this reduction in ERK1/2 activity was accompanied by the decrease in KGN cell migration, becoming significant at 10 and 20 µM (Figure 3B). A marked decrease in Matrigel invasion was also visible, even at a low concentration of

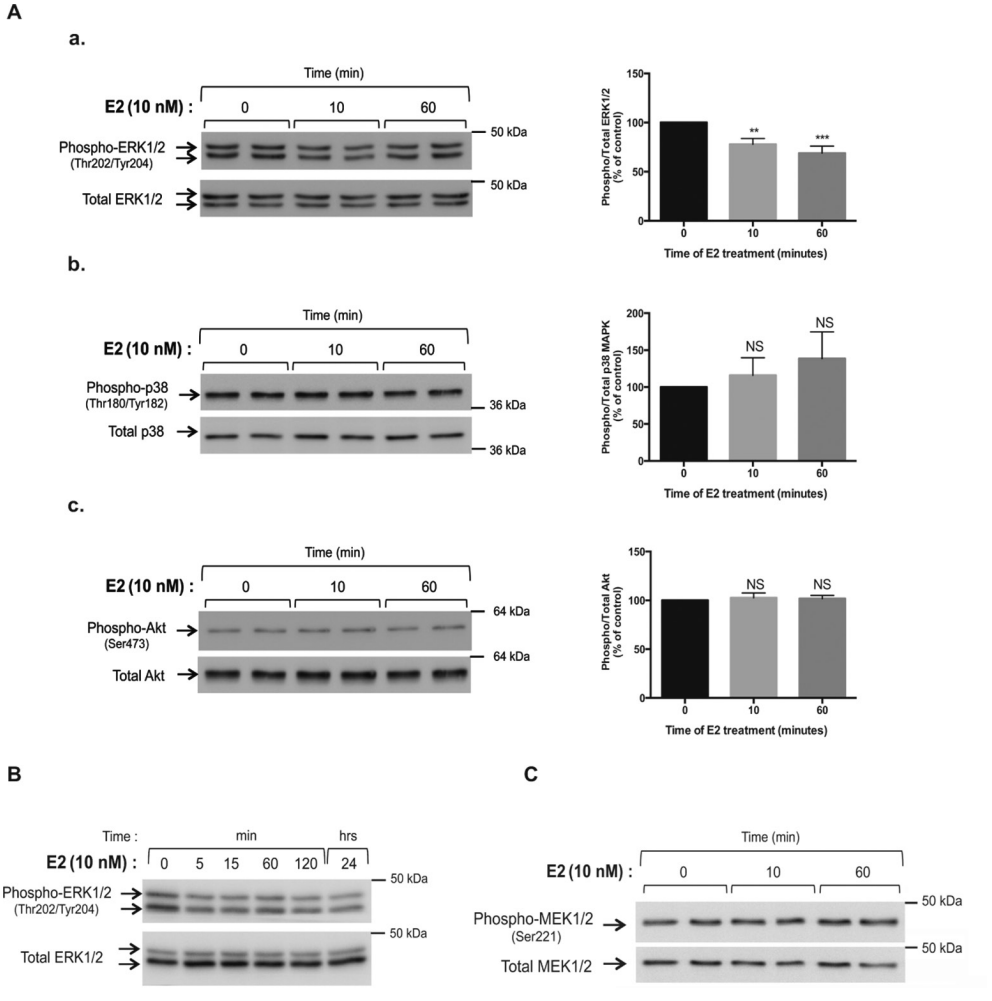

Figure 2. E2 specifically decreases the activity of ERK1/2 by non-genomic mechanisms in metastatic granulosa cells. (**A**) Analyses of the activity of MAPK and PI3K signaling pathways by western blot assays on whole cell lysates of KGN cells after 10 and 60 min of E2 treatment. (a) Expression levels of phospho- and total ERK1/2. (b) Expression levels of phospho- and total p38 MAPK. (c) Expression levels of phospho- and total Akt. The ratios of phosphorylated to total levels, which reflect protein kinase activity, were determined after quantification of band intensities. Graphs show the means ± SEM of at least three independent experiments. (**B**) Time-course study of phospho- and total ERK1/2 levels from 5 min to 24 h after a 10-nM E2 treatment. (**C**) Representative western blot assay of phospho- and total MEK levels in KGN cells with or without E2 treatment. Cells were treated by E2 for 15 min.

U0126 (Figure 3C). These results, thus, indicate that ERK1/2 signaling could drive the spreading of metastatic granulosa cells.

E2-induced ERK1/2 repression is not mediated by ERα or ERβ but it involves GPER1

To determine which ER mediates E2 actions in metastatic granulosa cells, we conducted a number of cell-based and molecular studies. First, we examined the expression of ERα and ERβ by immunofluorescence and found both receptors to be expressed in KGN cells (Figure 4A). We treated cells with agonists of ERα and ERβ, PPT (1,3,5-Tris(4-hydroxyphenyl)-4-propyl-1H-pyrazole) and DPN (2,3-bis(4-hydroxyphenyl)propionitrile), respectively, which are reported to mediate both non-genomic and nuclear E2 actions (28). None of these two agonists could reproduce the inhibitory action of E2 in KGN cells on migration and invasion capabilities as well as on ERK1/2 activity (Figure 4B–D). We also evaluated the effect of E2 on Matrigel invasion when cells were pretreated with specific ERα and ERβ antagonists, namely MPP dihydrochloride (1,3-*bis*(4-hydroxyphenyl)-4-methyl-5-[4-(2-piperidinylethoxy)phenol]-1H-pyrazole dihydrochloride; 10 nM) and PHTPP (4-[2-Phenyl-5,7-*bis*(trifluoromethyl)pyrazolo[1,5-*a*] pyrimidin-3-yl]phenol; 100 nM), respectively. None of these treatments could efficiently prevent E2 action in these cells (Figure 4E). Altogether, these data showed that neither ERα nor ERβ is involved in E2-induced repression on cell migration and invasion in these cells.

We next investigated the possibility that E2 could mediate its action via GPER1 (16). This receptor, which belongs to the GPCR family, is known to mediate E2 action by regulating the activity of PI3K and ERK1/2 pathways (16,29).

In line with previous observations in other cell lines (16,30), our confocal immunofluorescence microscopy studies revealed that in KGN cells GPER1 was present in the perinuclear region, indicating the preferential localization of the receptor in the cytoplasm (Figure 5Aa). Double immunostaining with an antibody recognizing calnexin, a reticulum endoplasmic marker, showed that GPER1 co-localized with this organelle (Figure 5Ab).

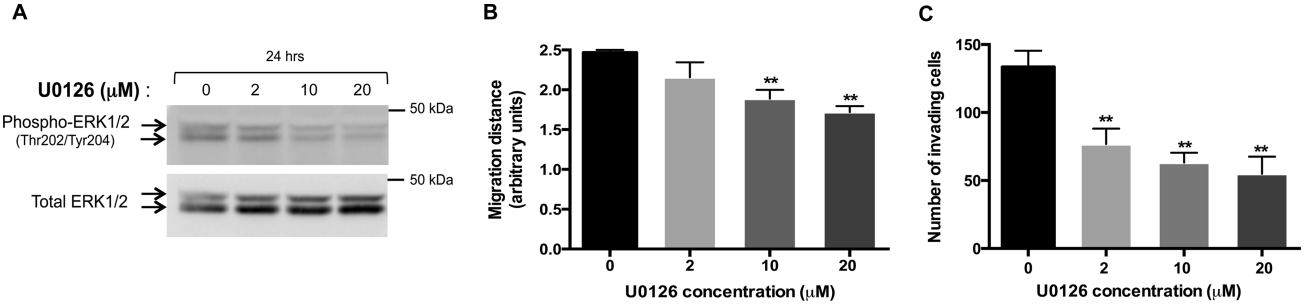

Figure 3. Pharmacological inhibition of ERK1/2 activity in KGN cells by U0126 leads to decreased cell migration and matrix invasion. (**A**) Analyses of ERK1/2 activity by western blot after a 24-h treatment by U0126 at different concentrations. The ratios of phospho- to total protein levels, after quantification of the band intensities for each sample, are indicated. (**B**) Bi-dimensional horizontal migration assays of KGN cells treated for 24 h with U0126. Shown are the means ± SEM of the migration distance from at least three experiments. (**C**) Matrigel invasion assays of KGN cells in transwell chambers. Cells were treated for 4.5 h with the indicated concentrations of U0126. Shown are the means ± SEM of the number of invading cells counted in photographed fields, as described in Materials and methods. $^{**}P < 0.01$ versus control.

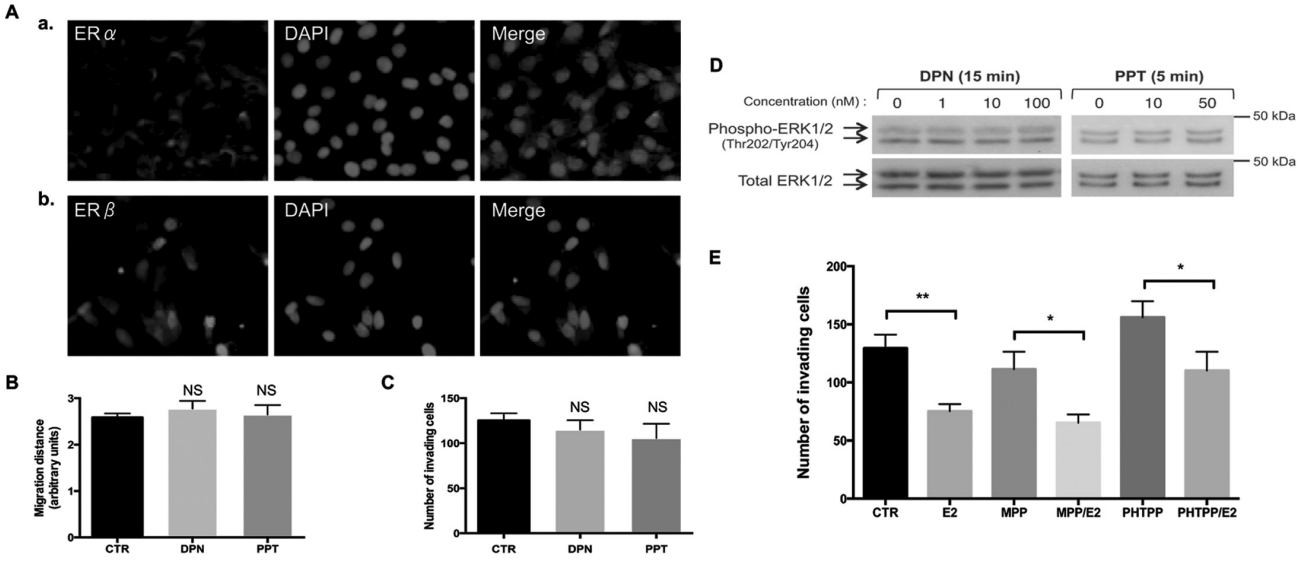

Figure 4. The effects of E2 in KGN cells are not mediated by ERα or ERβ. (**A**) Immunofluorescence studies showing (a) ERα and (b) ERβ expression in KGN cells. (**B**) Bi-dimensional horizontal migration assays of KGN cells treated for 24 h with the vehicle (CTR: DMSO), or with the agonists for ERβ (DPN, 10 nM) and for ERα (PPT, 10 nM). Quantification is shown as means ± SEM of the distance of migration, as described in Materials and methods. (**C**) Matrix invasion assays of KGN cells treated for 4.5 h with the vehicle (CTR), DPN (10 nM) or PPT (10 nM). The mean number ± SEM of invading cells per treatment group is shown in bar graphs. (**D**) Western blot assays of phospho- and total ERK1/2 levels in KGN cells after DPN or PPT treatment at different concentrations for the indicated times. (**E**) Matrigel invasion assays of KGN cells pretreated for 1 h with the vehicle (CTR), or the antagonists for ERα (MPP, 1,3-Bis(4-hydroxyphenyl)-4-methyl-5-[4-(2-piperidinylethoxy)phenol]-1H-pyrazole dihydrochloride, 10 nM) and for ERβ (PHTPP, 4-[2-Phenyl-5,7-*bis*(trifluoromethyl)pyrazolo[1,5-*a*]pyrimidin-3-yl]phenol, 100 nM) and treated for 4.5 h with E2 (10 nM). $^{*}P < 0.05$ versus control, $^{**}P < 0.01$ versus control; NS, not significant.

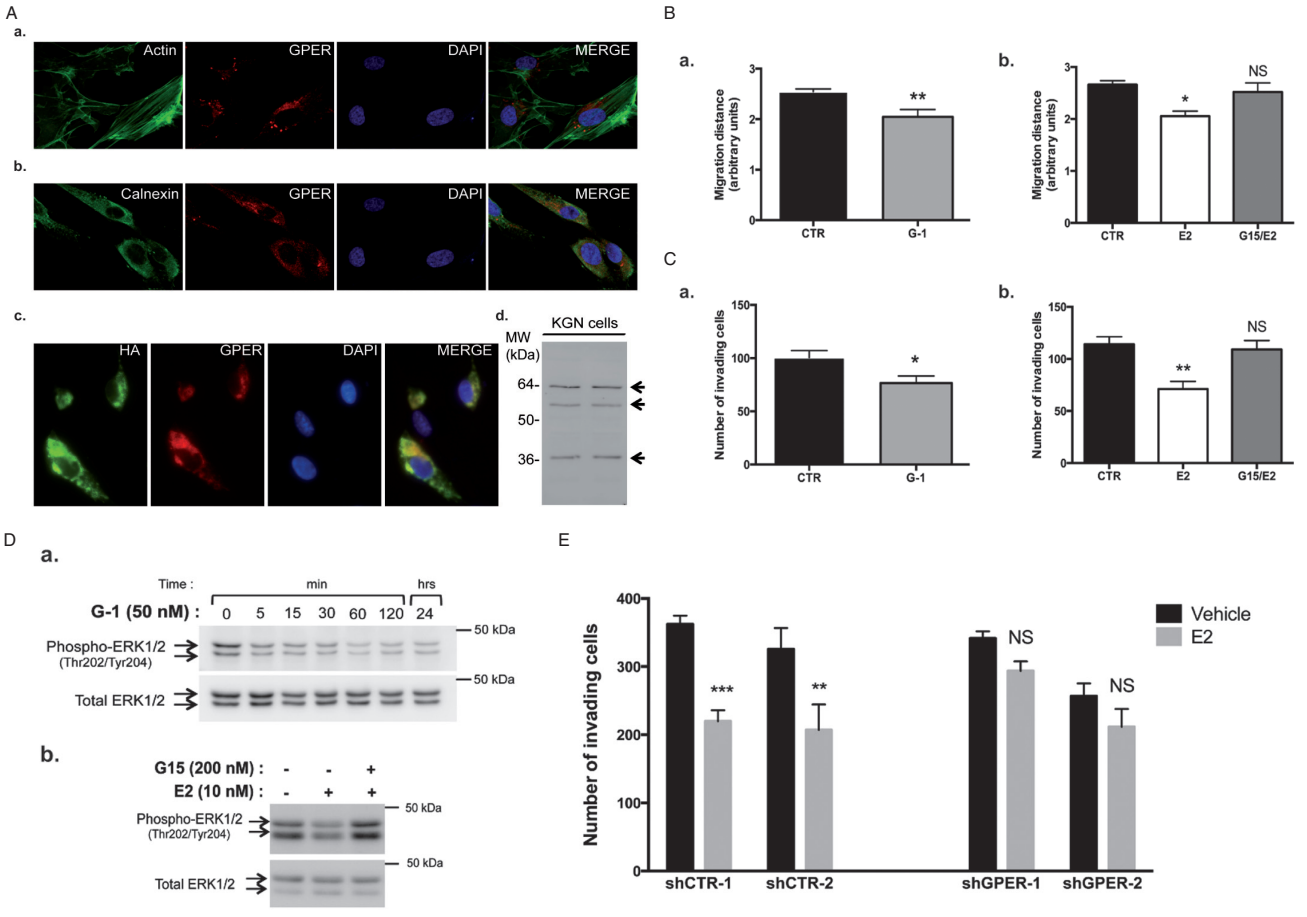

Figure 5. E2 mediates its action in metastatic granulosa cells via the GPER1 signaling pathway. (**A**) GPER1 expression in KGN cells. (a) Confocal immunofluorescence studies of GPER1 (red) with staining of the filamentous actin by phalloidin-fluorescein isothiocyanate (green) and of the nuclei with DAPI. In (b), double immunostaining of an endoplasmic reticulum (ER) marker, of calnexin (red) and of GPER1 (green). (c) Immunofluorescence studies on transiently transfected KGN cells expressing HA-GPER1 performed with antibodies against HA (green) and GPER1 (red, Sigma). In (d), western blot assays on two different samples of whole cell lysates performed with the LS4271 antibody. (**B**) Bi-dimensional horizontal migration assays of KGN cells treated for 24 h with either (a) the GPER1 agonist G-1 (50 nM) or (b) E2 preceded by pretreatment with the GPER1 antagonist G15 (200 nM) for 1 h. CTR, control (DMSO). Shown are the means ± SEM of the migration distance, determined as described in Materials and methods. (**C**) Matrigel invasion assays of KGN cells treated for 4.5 h with the vehicle (CTR: DMSO) and either (a) the GPER1 agonist G-1 (50 nM) or (b) pretreated with the GPER1 antagonist G15 (200 nM) prior to E2 treatment (10 nM). Shown are the means of the number of invading cells/field ± SEM, as described in Materials and methods. (**D**) Western blot assay of phospho- and total ERK1/2 levels in KGN cells, (a) at different time after G-1 treatment and (b) after a 1-h pretreatment with G15 followed by a 5-min E2 incubation. (**E**) Matrigel invasion assays of stable KGN cell lines wherein GPER1 is silenced by shRNAs. Two negative control (shCTR) and two shGPER1 clones were treated with the vehicle (CTR: DMSO) or with E2 (10 nM) for 4.5 h. Shown are the means of the number of invading cells/field ± SEM, as described in Materials and methods. *$P < 0.05$ versus control, **$P < 0.01$ versus control, ***$P < 0.001$ versus control; NS, not significant.

In cells expressing HA-tagged GPER1, a complete overlapping between anti-HA staining and two distinct commercial anti-GPER1 antibodies was observed, confirming the reliability of these antibodies (Figure 5Ac, and data not shown). Western blot assays to detect GPER1 in KGN cells yielded several bands (Figure 5Ad), as shown in other cell lines (31). The band at ~38–40 kDa corresponds to the theoretical molecular weight of the receptor, whereas the higher bands at ~57 and 64 kDa may correspond to *N*-glycosylated forms of GPER1.

To determine whether GPER1 could mediate the inhibitory E2 action on metastatic GCT cell migration and invasion, we took advantage of selective modulators of GPER1 activity, the agonist G-1 (32) and the antagonist G15 (33). G-1 treatment did not affect KGN cell growth (Supplementary Figure 2, available at *Carcinogenesis* Online), but it induced a ~20–30% decrease in their migration, as shown in bi-dimensional horizontal migration assays (Figure 5Ba). Pretreatment with the GPER1 antagonist G15 prior to E2 treatment totally abolished E2-induced repression on KGN cell migration (Figure 5Bb). We also assayed the effect of GPER1 signaling on extracellular matrix invasion. We found that G-1 significantly reduced Matrigel invasion, whereas pretreatment with G15 prior to incubation with E2 efficiently prevented the inhibitory action of E2 (Figure 5Ca and b). We then studied the possibility that GPER1 signaling could mediate E2 action and regulate ERK1/2 activity. To address this question, time course studies of ERK1/2 phosphorylation after treatment with G-1 were performed. The activity of ERK1/2 was consistently decreased from 5 min to 24 h (Figure 5Da), as observed with E2 (Figure 2Ba). In contrast, pretreatment of cells with G15 totally prevented E2-induced ERK1/2 repression (Figure 5Db).

To further ascertain the involvement of GPER1, we examined the effect of E2 treatment on the invasion capabilities of KGN cells wherein the expression of GPER1 has been silenced using shRNAs. The shRNA controls did not affect the cell response to E2, since the treatment reduced cell invasion by ≈30% (Figure 5E). In contrast, the inhibitory effect of E2 on cell invasion was lost in the two shGPER1 cell clones. Overall, these data support the involvement of GPER1 in mediating E2 action in metastatic granulosa cells.

GPER1 is expressed in GCTs at early and advanced stages of the disease

Collection of human sex-cord stromal tumors samples and preparation of TMAs provided us with the opportunity to analyse GPER1 expression in 59 adult GCTs. To confirm the diagnosis of adult-type GCTs, all samples were also tested for the presence of the *FOXL2* nucleotide C→G mutation at position 402 (Cys134Trp mutation), which is specifically found in this form of tumor (2,7). Only samples with mutated *FOXL2* were subsequently analysed for GPER1 expression. Clinical data including age at surgery, tumor stage, recurrence and duration of follow-up could be obtained for 29 of these patients. Median age at diagnosis was 50.5 years (24.3–75.1 years old). The follow-up of most patients was relatively short in duration (median: 1.9 years), and no patient died of her disease. Twenty-one samples were obtained from initial diagnosis (first surgery), whereas eight were from recurrent GCTs.

About 90% of GCTs expressed GPER1 (Supplementary Table 1, available at *Carcinogenesis* Online). Samples usually displayed more than 60% of immunostained cells, suggesting that a majority of tumoral granulosa cells displayed E2 receptivity through GPER1. GPER1 staining was essentially observed in the cytoplasmic compartment (Figure 6Ab). Interestingly, nuclear staining could also be found in a subset of tumors diagnosed at an early stage (Supplementary Table 1, available at *Carcinogenesis* Online).

There was no significant difference in the GPER1 immunoreactivity score between tumors collected at the time of either initial diagnosis or recurrence (Figure 6B). In addition, no significant correlation could be found between the stage of the tumor and the GPER1 immunoreactivity score ($P = 0.59$, data not shown). However, there was an inverse relationship between tumor size and GPER1 immunoreactivity score, with lower staining being observed in bigger tumors (Figure 6C; Pearson correlation $r = -0.38$; $P = 0.0431$).

Discussion

GCTs are characterized by their long natural history and their tendency to recur years after initial diagnosis. The main treatment is surgery, and the benefits of adjuvant, postoperative chemotherapy remain unclear. It is, thus, critical to uncover the molecular mechanisms involved in this pathogenesis in order to discover drugs that will efficiently treat patients. Although it was reported more than 2 decades ago that most GCTs produce high amounts of E2, the possible role of this hormone in this pathogenesis is still not clear. In this study, we found that E2 may play an important role in GCT progression by limiting metastasis spreading. Furthermore, we identified GPER1 as the receptor mediating E2 actions in these tumors.

Our cell-based studies with tumoral granulosa cells derived from primary tumors or from metastases showed that E2 had no effect on GCT cell growth. However, E2 significantly decreased migration and extracellular matrix invasion of metastatic granulosa cells. No such effects were observed with the primary tumor-derived granulosa cell line that does not have the capacity to migrate *in vitro*. Therefore, how estrogens would mediate their actions in metastatic granulosa cells was investigated. Because genomic E2 actions via ERs is not operative in GCT cells (14), we sought the possible contribution of non-genomic mechanisms. Indeed, these past years it has become apparent in cell-based studies but also *in vivo* that estradiol initiates non-genomic responses via ERs to regulate intracellular signaling pathways (for review see (15)). As these effects occur in a time frame (a few minutes) that is too rapid to be mediated by the biosynthesis of RNAs or new proteins, they can be distinguished from genomic actions. Importantly, our molecular studies of both MAPK and PI3K/Akt pathways revealed that E2 rapidly and specifically downregulated the phosphorylation levels of ERK1/2 in metastatic KGN cells. Aberrant overactivation of ERK1/2 has been reported in a wide array of cancers, including GCTs (27). ERK1/2 stimulates cell motility by regulating the expression and/or the activity of proteins involved in cell adhesion, cell motility and matrix remodelling (34). The present report indicates that this pathway is also crucial in regulating metastatic granulosa cell spreading, since its inhibition by either E2 or with a MEK1/2 inhibitor led to decreased KGN cell migration and extracellular matrix invasion.

The next step of our study was to determine which ER mediates E2 action in metastatic granulosa cells. Because our pharmacological studies with specific ER agonists and antagonists indicated that E2 actions were not ERβ- or ERα-mediated, we considered the contribution of the seven-transmembrane G protein-coupled receptor, GPER1. Whereas the rapid signaling events initiated by estrogens were initially ascribed solely to the classical estrogen receptors ERα and ERβ, during the past few years novel ER capable of mediating non-genomic actions have been identified such as GPER1 (35). In the present study, we report that this receptor was expressed in the endoplasmic reticulum region of metastatic granulosa cells, as described for other cell lines (16,30). To investigate the possibility that GPER1

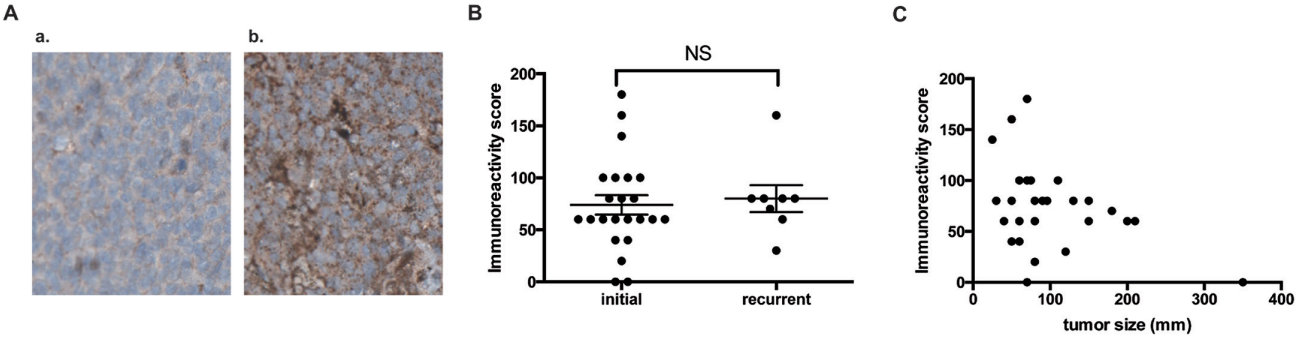

Figure. 6. GPER1 is expressed in adult GCTs. (**A**) Immunohistochemistry studies of GPER1 on TMAs of adult GCTs. Shown are tumors with no staining (a) and with moderate staining (b). Tissue sections are counterstained with hematoxylin (blue nuclear staining). (**B**) Comparison of the immunoreactivity score of GPER1 between samples recovered at initial diagnosis and during recurrence. The horizontal lines and error bars represent the means of immunoreactivity scores ± SEM, respectively. NS, not significant. (**C**) Pearson correlation analysis between GPER1 immunoreactivity score and tumor size ($r = -0.38$; $P = 0.0431$). Each dot represents the data collected from one patient.

could mediate estrogen effects in metastatic granulosa cells, we performed cell-based and molecular studies using selective agents that do not bind classical ERs but that targets GPER1, namely the G-1 agonist and the G15 antagonist. Treatment with G-1 treatment fully reproduced the described inhibitory effect of E2 in these cells, whereas pretreatment with G15 led to its complete suppression. Besides, GPER1 silencing using shRNAs led to the loss of E2 inhibitory action. Altogether, these experiments indicate that in metastatic GCT cells, E2 mediates its action through GPER1 and not by the classical ERs.

We presently do not know how E2 acts through GPER1 in metastatic granulosa cells. It is commonly admitted that stimulation of GPER1 activates epidermal growth factor receptor, leading to downstream activation of signaling molecules such as PI3K/Akt and ERK1/2 via Ras/Raf. Noteworthy, we observed that E2-induced repression of ERK1/2 activity occurred independently of Ras/Raf upstream signaling, since there was no change in the activity of MEK1/2 upon E2 treatment. Whereas the mechanisms underlying ERK1/2 regulation by E2 is not clear at present, we suspect that in these cancer cells E2 may regulate the activity of protein phosphatases dephosphorylating ERK1/2, such as MAPK phosphatases. Importantly, observations that GPER1 signaling leads to ERK1/2 repression have also been reported in vascular smooth muscle cells (36) and in the uterus (37). Additional molecular studies should bring clues to understand this alternative mode of GPER1 signaling.

Immunohistochemistry on TMA confirmed GPER1 expression in ~90% of GCTs collected at early or advanced stages of the disease, suggesting that E2 may well regulate this pathogenesis through GPER1 signaling. However, because there was an inverse relationship between the size of the tumor and GPER1 immunoreactivity, with bigger tumors expressing lower levels of GPER1, we suppose that E2 receptivity may decrease when the tumor grows in size. Because GCTs are relatively rare ovarian tumors that may recur years after surgical ablation (1), collecting GCT samples and clinical data from patients is challenging. In our study, patient follow-up was relatively short (~2 years) in view of the usual time frame of relapse (~10 years), and thus it was impossible to determine whether the level of GPER1 expression could be, as one may hypothesize from our study, associated with a better prognosis. On the other hand, each patient has a specific endocrine status in view of circulating E2 levels, menopausal status and use or not of hormone replacement therapy/contraceptives, and therefore such conclusions would require complex multiscale analyses integrating these parameters.

In conclusion, our work suggests that estradiol prevents the spreading of metastases from GCTs by repressing ERK1/2 activity via non-genomic mechanisms involving GPER1. Therefore, in contrast to other malignant tumors such as that of the breast (38,39), our cell-based studies suggest that GPER1 may act as a tumor suppressor in GCTs. The use of anti-estrogen therapy, including aromatase inhibitors is now common in the treatment of hormone-related cancers. It has also been tested on patients with recurrent GCTs (40). However, the therapeutic value of such a treatment in this disease has not been established yet, because only small-scale studies have been performed so far. In addition, the mechanisms of aromatase inhibitor action remain unclear. Indeed, besides lowering estrogen levels, aromatase inhibitors can lead to increase androgen levels, which could contribute to their therapeutic efficacy in androgen receptor positive cases (41). The present report reveals the interest of exploring in the near future the potential benefit of adjuvant treatments with selective modulators of GPER1 activity in patients with advanced GCTs. Further investigations on preclinical cell and animal models of GCT would be of great interest to uncover the complex picture of hormone actions in these endocrine cancer cells.

Supplementary material

Supplementary Table 1, Figures 1 and 2 and Supplementary Materials and methods can be found at http://carcin.oxfordjournals.org/

Funding

Fondation pour la Recherche Médicale (attributed to C.J.G., program “Espoirs de la recherche”); a Marie Curie International Reintegration grant within the 7th European Community Framework Programme (attributed to C.J.G., PIRG08-GA-2010–276970); the French National Cancer Institute, InCa (I.R.C.); a doctoral fellowship from the French ministry of Enseignement supérieur et Recherche (attributed to C.M.F.).

Acknowledgements

The authors would like to thank Drs Violaine Simon, David L’Hôte and Alice Pierre for their technical help and Eva Cabet from the Imaging Facility of the Functional and Adaptive Biology Unit for her help in confocal microscopy studies.
Conflict of Interest Statement: None declared.

References

1. Pectasides, D. et al. (2008) Granulosa cell tumor of the ovary. Cancer Treat. Rev., 34, 1–12.
2. Stuart, G.C.E. et al. (2011) 2010 Gynecologic Cancer InterGroup (GCIG) consensus statement on clinical trials in ovarian cancer: report from the Fourth Ovarian Cancer Consensus Conference. Int. J. Gynecol. Cancer Off. J. Int. Gynecol. Cancer Soc., 21, 750–755.
3. Shah, S.P. et al. (2009) Mutation of FOXL2 in granulosa-cell tumors of the ovary. N. Engl. J. Med., 360, 2719–2729.
4. Kim, J.H. et al. (2011) Differential apoptotic activities of wild-type FOXL2 and the adult-type granulosa cell tumor-associated mutant FOXL2 (C134W). Oncogene, 30, 1653–1663.
5. Benayoun, B.A. et al. (2010) Functional exploration of the adult ovarian granulosa cell tumor-associated somatic FOXL2 mutation p.Cys134Trp (c.402C>G). PLoS One, 5, e8789.
6. Fleming, N.I. et al. (2010) Aromatase is a direct target of FOXL2: C134W in granulosa cell tumors via a single highly conserved binding site in the ovarian specific promoter. PLoS One, 5, e14389.
7. Rosario, R. et al. (2012) The transcriptional targets of mutant FOXL2 in granulosa cell tumours. PLoS One, 7, e46270.
8. Maillet, D. et al. (2014) Impact of a second opinion using expression and molecular analysis of FOXL2 for sex cord-stromal tumors. A study of the GINECO group & the TMRO network. Gynecol. Oncol., 132, 181–187.
9. Petraglia, F. et al. (1998) Inhibin B is the major form of inhibin/activin family secreted by granulosa cell tumors. J. Clin. Endocrinol. Metab., 83, 1029–1032.
10. Rey, R.A. et al. (1996) Antimüllerian hormone as a serum marker of granulosa cell tumorsof the ovary: comparative study with serum alpha-inhibin and estradiol. Am. J. Obstet. Gynecol., 174, 958–965.
11. Jamieson, S. et al. (2012) Molecular pathogenesis of granulosa cell tumors of the ovary. Endocr. Rev., 33, 109–144.
12. Schomberg, D.W. et al. (1999) Targeted disruption of the estrogen receptor-alpha gene in female mice: characterization of ovarian responses and phenotype in the adult. Endocrinology, 140, 2733–2744.
13. Couse, J.F. et al. (2005) Estrogen receptor-beta is critical to granulosa cell differentiation and the ovulatory response to gonadotropins. Endocrinology, 146, 3247–3262.
14. Chu, S. et al. (2004) Transrepression of estrogen receptor beta signaling by nuclear factor-kappab in ovarian granulosa cells. Mol. Endocrinol. Baltim. Md, 18, 1919–1928.

15. Boonyaratanakornkit, V. et al. (2007) Receptor mechanisms mediating non-genomic actions of sex steroids. Semin. Reprod. Med., 25, 139–153.
16. Revankar, C.M. et al. (2005) A transmembrane intracellular estrogen receptor mediates rapid cell signaling. Science, 307, 1625–1630.
17. Nishi, Y. et al. (2001) Establishment and characterization of a steroidogenic human granulosa-like tumor cell line, KGN, that expresses functional follicle-stimulating hormone receptor. Endocrinology, 142, 437–445.
18. Van den Berg-Bakker, C.A. et al. (1993) Establishment and characterization of 7 ovarian carcinoma cell lines and one granulosa tumor cell line: growth features and cytogenetics. Int. J. Cancer J. Int. Cancer, 53, 613–620.
19. Jamieson, S. et al. (2010) The FOXL2 C134W mutation is characteristic of adult granulosa cell tumors of the ovary. Mod. Pathol. Off. J. U. S. Can. Acad. Pathol. Inc, 23, 1477–1485.
20. Zhang, H. et al. (2000) Characterization of an immortalized human granulosa cell line (COV434). Mol. Hum. Reprod., 6, 146–153.
21. Giretti, M.S. et al. (2008) Extra-nuclear signalling of estrogen receptor to breast cancer cytoskeletal remodelling, migration and invasion. PLoS One, 3, e2238.
22. Guigon, C.J. et al. (2008) Regulation of beta-catenin by a novel non-genomic action of thyroid hormone beta receptor. Mol. Cell. Biol., 28, 4598–4608.
23. Ray-Coquard, I. et al. (2010) Management of rare ovarian cancers: the experience of the French website "Observatory for rare malignant tumours of the ovaries" by the GINECO group: interim analysis of the first 100 patients. Gynecol. Oncol., 119, 53–59.
24. Filardo, E.J. et al. (2002) Estrogen action via the G protein-coupled receptor, GPR30: stimulation of adenylyl cyclase and cAMP-mediated attenuation of the epidermal growth factor receptor-to-MAPK signaling axis. Mol. Endocrinol., 16, 70–84.
25. Stoica, G.E. et al. (2003) Estradiol rapidly activates Akt via the ErbB2 signaling pathway. Mol. Endocrinol. Baltim. Md, 17, 818–830.
26. Takahashi, M. et al. (2008) Bone morphogenetic protein 6 (BMP6) and BMP7 inhibit estrogen-induced proliferation of breast cancer cells by suppressing p38 mitogen-activated protein kinase activation. J. Endocrinol., 199, 445–455.
27. Steinmetz, R. et al. (2004) Mechanisms regulating the constitutive activation of the extracellular signal-regulated kinase (ERK) signaling pathway in ovarian cancer and the effect of ribonucleic acid interference for ERK1/2 on cancer cell proliferation. Mol. Endocrinol., 18, 2570–2582.
28. Zhang, G. et al. (2009) Estrogen receptor beta functions through non-genomic mechanisms in lung cancer cells. Mol. Endocrinol. Baltim. Md, 23, 146–156.
29. Filardo, E.J. et al. (2000) Estrogen-induced activation of Erk-1 and Erk-2 requires the G protein-coupled receptor homolog, GPR30, and occurs via trans-activation of the epidermal growth factor receptor through release of HB-EGF. Mol. Endocrinol., 14, 1649–1660.
30. Otto, C. et al. (2008) G protein-coupled receptor 30 localizes to the endoplasmic reticulum and is not activated by estradiol. Endocrinology, 149, 4846–4856.
31. Sandén, C. et al. (2011) G protein-coupled estrogen receptor 1/G protein-coupled receptor 30 localizes in the plasma membrane and traffics intracellularly on cytokeratin intermediate filaments. Mol. Pharmacol., 79, 400–410.
32. Bologa, C.G. et al. (2006) Virtual and biomolecular screening converge on a selective agonist for GPR30. Nat. Chem. Biol., 2, 207–212.
33. Dennis, M.K. et al. (2009) *In vivo* effects of a GPR30 antagonist. Nat. Chem. Biol., 5, 421–427.
34. Huang, C. et al. (2004) MAP kinases and cell migration. J. Cell Sci., 117, 4619–4628.
35. Prossnitz, E.R. et al. (2011) The G-protein-coupled estrogen receptor GPER in health and disease. Nat. Rev. Endocrinol., 7, 715–726.
36. Li, F. et al. (2013) Activation of GPER Induces Differentiation and Inhibition of Coronary Artery Smooth Muscle Cell Proliferation. PLoS One, 8, e64771.
37. Gao, F. et al. (2011) GPR30 activation opposes estrogen-dependent uterine growth via inhibition of stromal ERK1/2 and estrogen receptor alpha (ERα) phosphorylation signals. Endocrinology, 152, 1434–1447.
38. Lappano, R. et al. (2014) GPER function in breast cancer: an overview. Front. Endocrinol. (Lausanne)., 5, 66.
39. Filardo, E.J. et al. (2012) Minireview: G protein-coupled estrogen receptor-1, GPER-1: its mechanism of action and role in female reproductive cancer, renal and vascular physiology. Endocrinology, 153, 2953–2962.
40. Sommeijer, D.W. et al. (2013) Hormonal treatment in recurrent and metastatic gynaecological cancers: a review of the current literature. Curr. Oncol. Rep., 15, 541–548.
41. Campagnoli, C. et al. (2013) Postmenopausal breast cancer, androgens, and aromatase inhibitors. Breast Cancer Res. Treat., 139, 1–11.